

UC Riverside

UCR Honors Capstones 2019-2020

Title

The Effect of Different Surfactants on the Photostability of Avobenzone in Sunscreens

Permalink

<https://escholarship.org/uc/item/0jj625d7>

Author

Cutuli, Miles

Publication Date

2020-04-01

Data Availability

The data associated with this publication are within the manuscript.

By

A capstone project submitted for
Graduation with University Honors

University Honors
University of California, Riverside

APPROVED

Dr.
Department of

Dr.
Department of

Dr. Richard Cardullo, Howard H Hays Jr. Chair, University Honors

Abstract

Table of Contents

- I. Introduction
- II. Materials and Methods
- III. Results and Discussion
- IV. Conclusion
- V. Acknowledgements
- VI. References

Introduction

The ultraviolet (UV) radiation emitted from the sun has the potential to facilitate harmful photoreactions within the epidermis and dermis from the interaction of UV photons with chromophores (urocanic acid, flavins, lipids, collagen, DNA) in the skin. Short term consequences include erythema and immunomodulation, while long-term exposure can promote photoaging and carcinogenesis. Commercial sunscreens can prevent these harmful consequences because they contain UV filter molecules that form a layer on the skin surface that minimizes the penetration of UV photons into skin. Therefore, the application and development of stable UV filter molecules is of great interest because of their proactive approach on alleviating the damaging effects of solar UV radiation on organic and material systems.

UV light emitted from the sun is subcategorized based on the wavelength emitted; UVA (320-450 nm), UVB (280-320 nm) and UVC (<280 nm). Unlike UVA and UVB, UVC is primarily blocked by the ozone layer and does not typically reach earth's surface. UVB causes sunburn, and until recently sunscreens only afforded protection against these rays solely to prevent it. Researchers have now determined that UVA actually penetrates more deeply into the dermis than UVB, and it is considered the primary cause of the visible signs of aging. Today, both UVB and UVA are considered carcinogenic.

With the realization that UVA elicits negative photochemical reactions within the skin, sunscreens have been reformulated to include UVA-blocking UV filters. Avobenzene (**AV**, 4-*tert*-butyl-4'-methoxydibenzoylmethane) is the only carbon-based (or as it is called in the industry "chemical") molecule approved by the Food and Drug Administration (FDA) to absorb UVA photons in sunscreens. AV functions as a UV filter molecule in sunscreen by absorbing and expelling UV energy through the transition of electrons between the singlet ground, singlet

excited, and triplet excited states. Unfortunately, the molecule is highly photolabile. Specifically, previous research has shown that during UV irradiation, AV undergoes a photochemical reaction from its UVA absorbing tautomer (chelated enol) to its UVC absorbing diketone tautomer. This leads to a concomitant loss in the efficacy of the sunscreen to

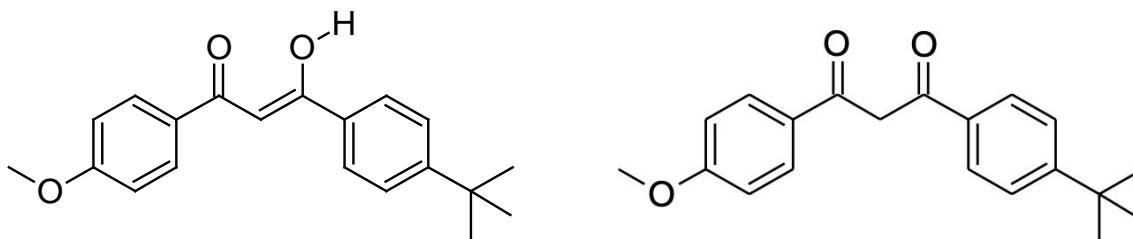


Figure 1 AV: unchelated keto-enol isomer (left) and diketone isomer (right).

block UVA light and its effectivity to protect against harmful UVA exposure. The chelated keto-enol form absorbs in the UVA region due to its conjugated carbonyl-ethylene. The exact reaction mechanism of the tautomerization of the chelated keto-enol form to the diketone forms remains unknown and only a potential mechanism may be theoretically suggested. Interestingly, observation has demonstrated this mechanism of tautomerization is highly dependent on the environment of AV in solution. In polar, protic solvents AV does not readily tautomerize and is exclusively preserved in the chelated keto-enol form which offers photo-protection against UVA radiation. In non-polar and polar, aprotic solvents AV is observed to readily tautomerize into the diketone isomer. Such observations suggest the ability of hydrogen bonding to effectively stabilize AV and minimize tautomerization given its polar, protic characteristics. In principle

water would be an ideal solvent for AV because it offers biocompatibility with the epidermis and dermis compared to methanol which displays toxic properties. Unfortunately, AV exhibits hydrophobic characteristics and precipitates out of solution. Additionally, water would not provide a stable vehicle for water-resistant sunscreens for the consumer.

This project had two goals. First, to explore that nature of hydrogen bonding in the photostabilization of AV in a more commercially viable formulation, we proposed to study if surfactants could improve stabilization of the chelated-enol tautomer of the molecule.

Amphipathic molecules are a reasonable class of molecules to investigate because they contain both hydrophobic and hydrophilic regions, to promote favorable interactions with the solvent and solute simultaneously. The use of surfactants, amphipathic molecules, in solution may offer plausible observations because they act in conjunction with water as a favorable environment to stabilize AV. The objective of this project is to understand how surfactants can contribute in creating a favorable soluble environment to stabilize AV in its chelated keto-enol isomer. The second goal was to explore the effect of UV radiation on skin cell integrity using the technique of two-photon fluorescence imaging. Eventually, we want to use the knowledge gained about stabilizing AV to see if new formulations can provide better *in vivo* protection for actual human skin cells.

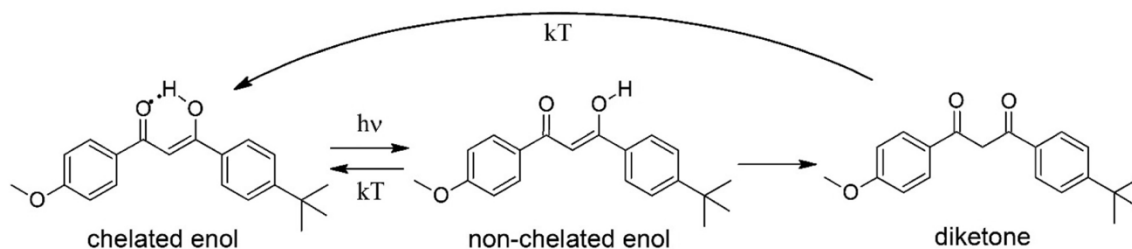


Figure 2 Tautomerization of AV from the stable chelated (keto)-enol form to the diketone form by the non-chelated enol intermediate, under UVA irradiation. *Photochem. Photobiol. Sci.*, 2020,19, 390-398

Materials and Methods

All reagents used were purchased commercially. AV was supplied by Merck Consumer Care Inc. (Memphis, TN). All solvents and surfactants were supplied by Sigma-Aldrich with a purity of >99%. The surfactants used include cetrimonium bromide (CTAB), trimethylammonium bromide (TTAB), sodium dodecylbenzenesulfonate (SDBS), sodium laurate (SL), and sodium dodecyl sulfate (SDS). The solvents used include cyclohexane, methanol, ethylene, glycol, and acetonitrile. MilliQ water was used as a solvent for surfactants and AV in solution.

Dilute solutions of 6 μM AV were made in various solvents such as methanol and cyclohexane. Solutions of AV in water and surfactants were made using the re-precipitation method. This method promoted the dissolving of AV in water by initially dissolving it in methanol and later allowing for its evaporation because of its low boiling point compared to water. Specifically, 200 μL of 10 mM AV in methanol was dissolved into a 10 mL solution of water and surfactant. Each sample of solution was allowed to sit for 45 minutes to allow for evaporation of the methanol, leaving a dissolved AV in solution with water and surfactant. Irradiation and fluorescence experiments of AV in surfactant solutions were created based on the critical micelle concentration of the respective surfactant. Notably, surfactants are characterized as amphipathic molecules that decrease the surface tension between a liquid and an adjacent entity; they are commonly used as detergents and soaps to remove colloids from surfaces. Their nonpolar tail and polar head are thought to interact with AV and the solvent, respectively, to minimize interaction with aggregates and increase stabilization. Surfactants have a unique property known as the critical micelle concentration (CMC), which refers to the minimum concentration of surfactant needed for the molecules to form a spherical structure in water. The

CMC is distinct for each surfactant and surfactant concentrations will be tested above and below this value to examine how CMC may play a role in the photostability of AV. The concentration of surfactants prepared include CTAB (2 mM), TTAB (8 mM), SDBS (5 mM), SL (42 mM). SDS was examined in its ability to form a micelle based on a varying concentration above and below the CMC (2 mM, 4 mM, 6 mM, 8 mM, 10 mM, 12 mM, 15 mM, 20 mM). The solution of AV and surfactant were stored in the dark for 24 hours to allow for micelle encapsulation and minimize UVA exposure prior to irradiation.

UV irradiation was performed and simulated by a solar simulator (Model 16S, 150 W, Solar Light Company, Glenside, PA). The UV light emitted comprised of 30 mW UVA and 1 mW UVB to mimic ≈ 10 minutes of noonday summer sun in North America. This is in exceptional consistency with the UVA:UVB ratio of standard solar spectrum ASTM. Irradiation of 56 s is equivalent to 1 minimal erythemal dose (MED) at 22 mJ cm^{-2} UVB and 660 mJ cm^{-2} UVA. Each sample was housed in a cuvette of 3.2 mL and stirred consistently throughout irradiation to ensure homogenous UV exposure. Trials were performed in duplicates at $t = 0 \text{ s}$, 60 s, 300 s, 600 s, 1200 s, and 2400 s ($\pm 0.2 \text{ s}$). Absorption spectra of solutions were documented and characterized at each time interval by a Cary-500 absorption spectrophotometer. Spectra were normalized and subtracted from a sample spectrum to adjust for minor variations and to determine the remaining concentration of AV in the enol form over the irradiation period. The resulting data was plotted on graphs of absorbance (normalized) vs time in order to illustrate the rate of enol decay to the diketone formation over time. The fluorescence lifetime of AV was recorded using a picosecond streak camera, Streakscope Hamamatsu C4334. The excitation pulses at 320 nm were generated by a Ti:sapphire regenerative amplified laser and optical parametric amplifier. Fluorescence spectra of solutions were recorded by a QuantaMaster 8000

(Horiba, Irvine, CA). Solutions were consistently stirred throughout experimentation and data collection of fluorescence. Additionally, two-photon fluorescence instrumentation at the Laboratory for Fluorescence Dynamics at UC Irvine was used to image the skin during periods of irradiation. The images are processed utilizing a computer software, SimFCS, to isolate specific regions of cell and lipid membranes from the stratum corneum to the stratum basale.

Solvent	Absorption λ_{\max} (nm)	Emission λ_{\max} (nm)	f_{Enol}^a (std dev)	τ_{fl} (ps)
Cyclohexane	352	402	0.03 (0.01)	<7
Methanol	360	410	0.99 (0.00)	<7
Ethylene glycol	362	414	0.96 (0.00)	—
Water	368	423	0.35 (0.02)	—
SDS (20 mM)	363	419	0.96 (0.01)	18 ps ($a = 0.9$) 125 ps ($a = 0.1$)
SDS (15 mM)	363	417	0.97 (0.01)	—
SDS (12 mM)	363	419	0.96 (0.00)	—
SDS (10 mM)	363	419	0.94 (0.01)	—
SDS (8 mM)	363	421	0.81 (0.06)	—
SDS (6 mM)	363	424	0.87 (0.02)	—
SDS (4 mM)	401	422	0.79 (0.19)	—
SDS (2 mM)	363	424	0.67 (0.17)	—
CTAB (2 mM)	356	—	0.82 (0.02)	—
SDBS (5 mM)	361	—	0.96 (0.02)	—
SL (42 mM)	361	—	0.93 (0.01)	—
TTAB (8 mM)	361	—	0.91 (0.04)	—

^a Fraction of enol remaining after 1200 s^{-1} (0.5 J cm^{-2} UVB, 14.1 J cm^{-2} UVA).

Figure 3 Spectroscopy parameters of AV in various solvents. f_{Enol}^a measures the normalized fraction of enol isomer present after 1200 s of irradiation. *Photochem. Photobiol. Sci.*, 2020,19, 390-398

Results and Discussion

The insolubility of AV in water was a major concern because of its tendency to form aggregates rather than homogeneously dissolve in solution. The surfactant SDS was utilized to understand how a varying surfactant concentration could affect the formation of a micelle and how that may alter the tautomerization of the enol to the diketone. Specifically, Figure 4 illustrates the absorption spectrum of AV with an increasing concentration of SDS. Aggregation of AV in relation to the CMC (8 mM) of SDS demonstrates greater aggregation at concentrations below the CMC. A broad peak at 2 mM, ranging from 340 nm to 400 nm correlates to the aggregation of AV throughout the solution, decreasing its photostability. Increasing the concentration above the CMC, the peak at 20 mM is much sharper and taller exemplifying the ability of SDS to stabilize AV and absorb at a greater intensity. Additionally, the sharp peak is

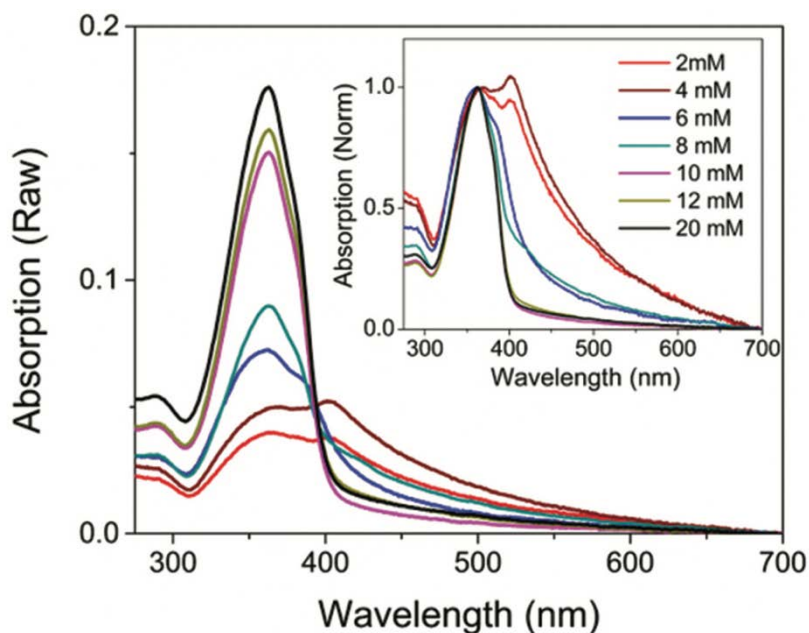


Figure 4 AV in SDS solution among varying concentrations. Distinction between the sharpness and intensity of the peak above the CMC (8 mM). *Photochem. Photobiol. Sci.*, 2020,19, 390-398

indicative of a homogeneous solution where AV was readily able to dissolve in water by interacting with SDS. The absorption and fluorescence experiments of AV in SDS solution indicates that the formation of micelles prompts the AV molecules to solubilize in solution rather than aggregate. Given the amphipathic nature of surfactants, micelle formation results in the encapsulation of AV molecules via an interaction between the hydrophobic carbon chains and the nonpolar, hydrophobic groups of AV. It is notable to recognize the stability of AV in surfactant is a consequence of the intermolecular force solute-solve interaction between water and AV. Specifically, the interaction between water and AV promotes intermolecular hydrogen-bonding and greater stability of the enol isomer. This is consistent with the high absorption values of AV in methanol because of its intermolecular hydrogen-bonding capability characterized by being a polar, protic solvent like water. Figure 6 is also consistent with the notion of micelle formation stabilizing the enol isomer because the Anisotropy, the direction and position of the molecule, exhibits an increase above the CMC of SDS. These data suggest AV is encapsulated by the micelle, but AV still consistently interacts with the solvent via hydrogen bonding. AV likely resides in the micelle near the polar heads of the surfactant to favorably interact with the solvent.

Time-resolved fluorescence measurements collected coincide with the scheme that AV interacts with the polar groups of the micelle and the intermolecular hydrogen bonding of water. Figure 5 illustrates a shorter-lived excitation lifetime of methanol when compared to the lifetime of 20 mM SDS. A longer-lived fluorescence lifetime corresponds to the decreased heat dissipation of AV through a mechanism related to the polar microenvironment of the solute. The formation of the SDS micellar structure facilitates the stability of AV through hydrogen bonding. Increased stability of AV is analogous to a longer period of time to maintain the enol isomer

because the solute experiences less energy release following excitation, decreasing the possibility of isomerization from the enol to the diketone form.

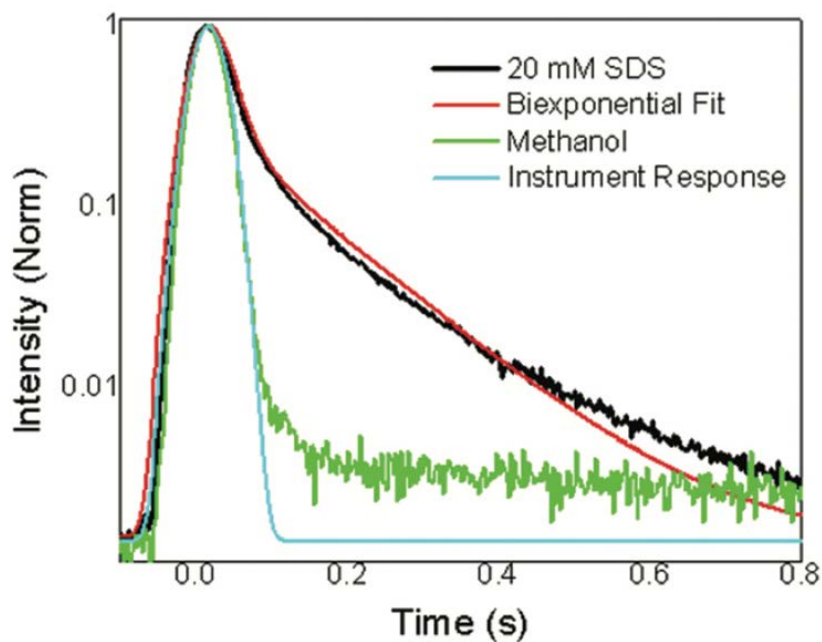


Figure 5 Fluorescence lifetime of AV in different environments. 20 mM SDS exhibits a longer lifetime compared to methanol, demonstrating a more stable configuration. *Photochem. Photobiol. Sci.*, 2020,19, 390-398

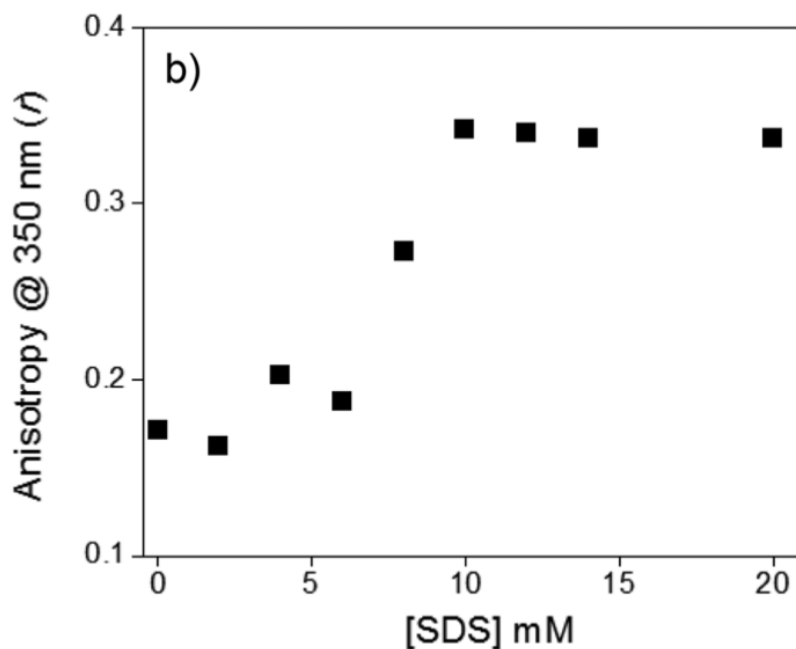


Figure 6 The Anisotropy, position and directional dependence, of different concentrations of SDS at the λ_{\max} of the enol. *Photochem. Photobiol. Sci.*, 2020,19, 390-398

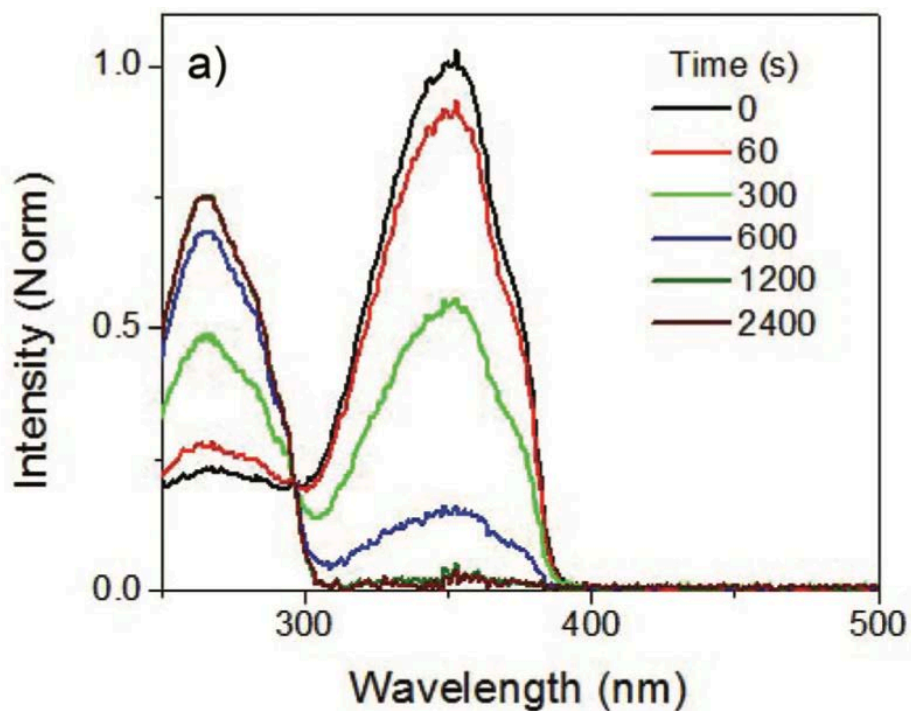


Figure 7 The absorption of 6 μM AV in *cyclohexane* over a 2400 s period of irradiation. *Photochem. Photobiol. Sci.*, 2020,19, 390-398

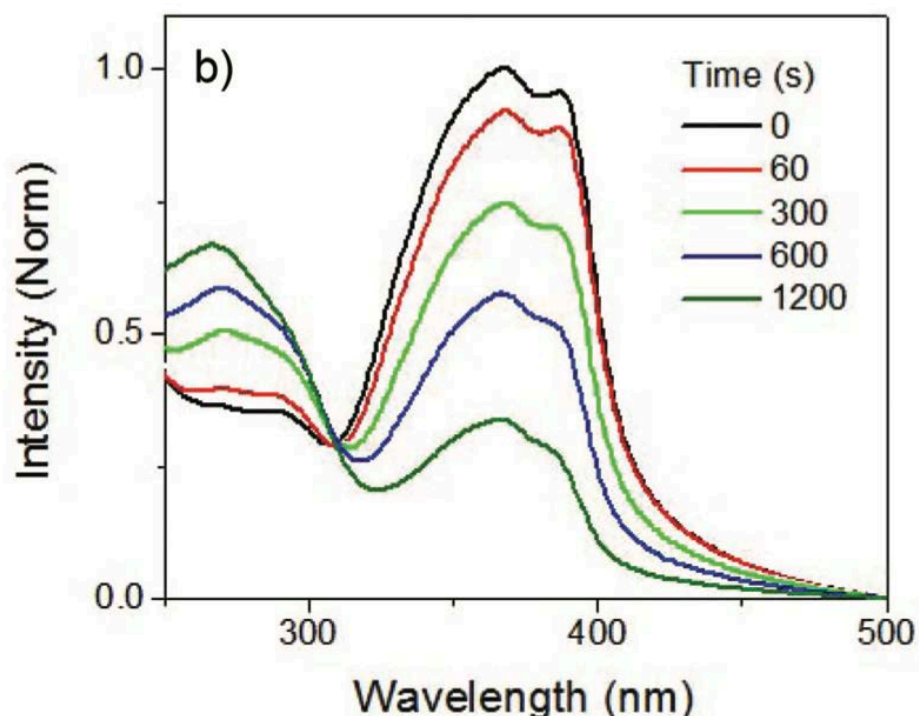


Figure 8 The absorption of 6 μM AV in *water* over a 2400 s period of irradiation. *Photochem. Photobiol. Sci.*, 2020,19, 390-398

AV undergoes a period of degradation in which it tautomerizes from the keto-enol form to the diketone form over long-term periods of UVA exposure. Cyclohexane is a non-polar solvent that dissolves AV, but exposure to UVA radiation leads to the degradation of AV in the enol form. Figure 7 illustrates the lack of photostabilizing characteristics of cyclohexane because the molecule rapidly tautomerizes. This is consistent with previous data suggesting polar, protic solvents exhibiting hydrogen bonding between the solute and solvent. Instead, cyclohexane does not exhibit the properties of intermolecular hydrogen bonding which is evident in the formation of the diketone form at 270 nm. The diminished intensity of the peak at 360 nm and the increase in intensity of the peak at 270 nm is consistent with the enol isomer and diketone isomer, respectively. AV exhibits a near 100% loss of efficacy in absorption intensity over 2400 s while in cyclohexane.

In aqueous solvents, AV exhibits a similar degradation pattern when compared to cyclohexane as the solvent. Over 2400 s, the absorption of the enol decreases by $\approx 60\%$ demonstrating a weak microenvironment for enol stabilization, instead promoting the formation of the diketone isomer. While water typically exhibits intermolecular hydrogen bonding interactions with the solute, there is no observation to support the formation of hydrogen bonds. The low solubility of AV in water facilitates the aggregation of colloidal AV leading to intermolecular interactions between neighboring AV molecules. Such interactions disrupt the ability of water to form hydrogen bonds with AV, prompting its tautomerization to the diketone form and losing its photoprotective capabilities. Figure 8 supports these findings and highlights the importance of AV dissolving in solvent to avoid aggregation and intermolecular interactions between nearby AV molecules.

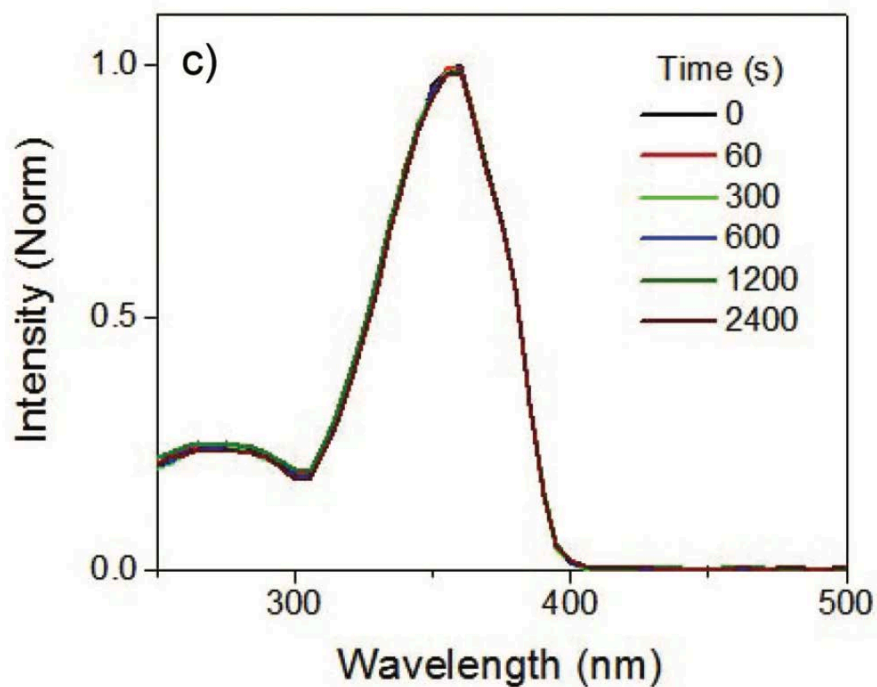


Figure 9 The absorption of 6 μM AV in *methanol* over a 2400 s period of irradiation. *Photochem. Photobiol. Sci.*, 2020,19, 390-398

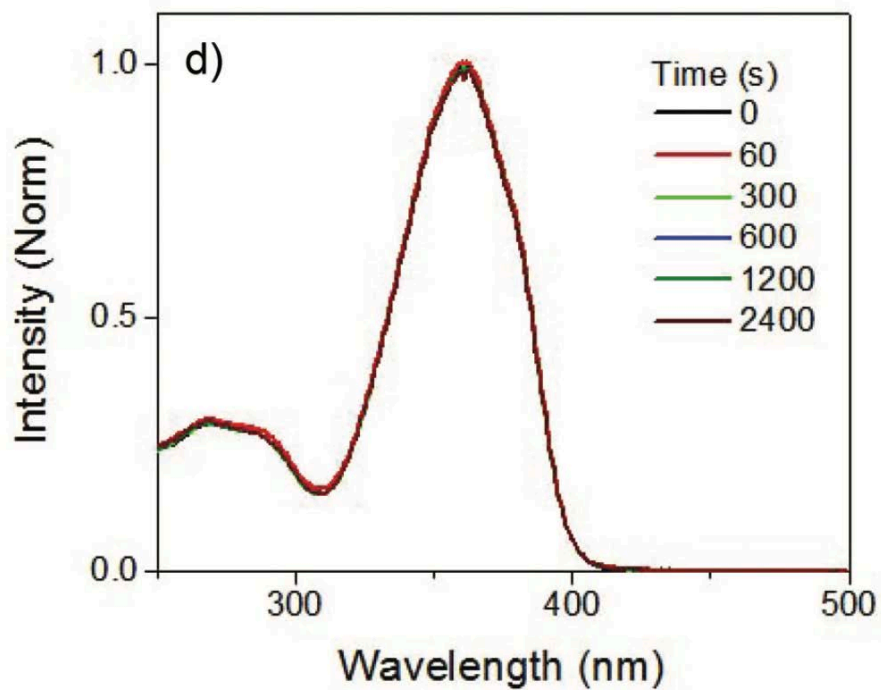


Figure 10 The absorption of 6 μM AV in 20 mM SDS over a 2400 s period of irradiation. *Photochem. Photobiol. Sci.*, 2020,19, 390-398

Methanol is classified as a polar, protic solvent because of its polar alcohol group and its tendency to hydrogen bond with certain solutes. Figure 9 illustrates the high absorption intensity of the enol isomer because of minimal formation and increase in the peak intensity corresponding to the diketone isomer. The solubility of AV in methanol alongside the intermolecular hydrogen bonding manifest into a very stable enol isomer, only degrading 1%. While methanol is effective in stabilizing AV and maintaining a high photoabsorption, it is associated with toxic characteristics making it undesirable as a practical ingredient in sunscreen. Acknowledging the importance of biocompatible is essential in ensuring the safety and well-being of commercial consumers of sunscreens. A prospective alternative involves the integration of surfactants such as SDS because of their photostabilizing effects. Figure 10 describes the stability of AV in 20 mM SDS, degrading 4% in efficacy over 2400 s. These results parallel the observations in stability of AV in methanol, supporting the potential use of SDS as a component in an AV formulation. Additionally, the biocompatible nature of SDS as a surfactant contributes to its potential as an alternative photostabilizer when compared to methanol or other toxic solvents.

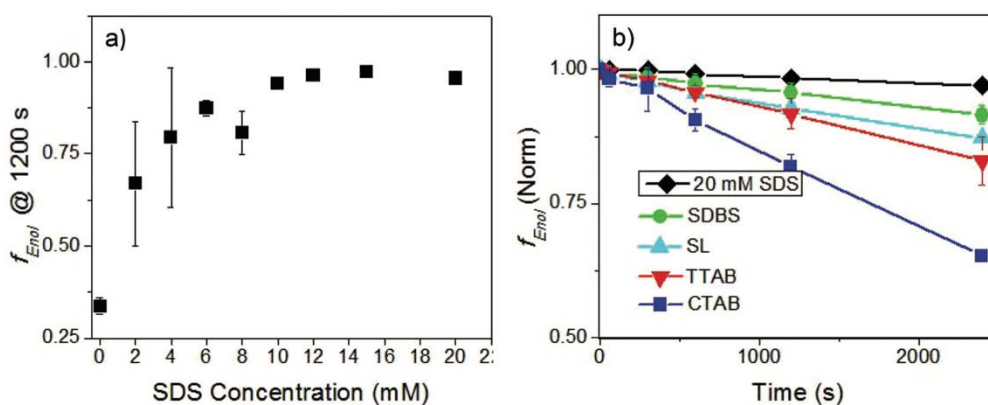


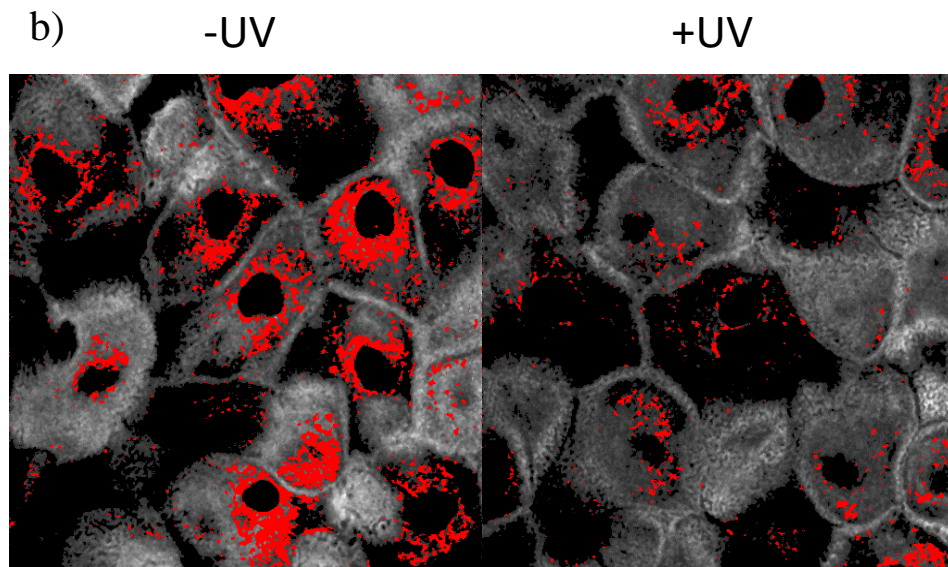
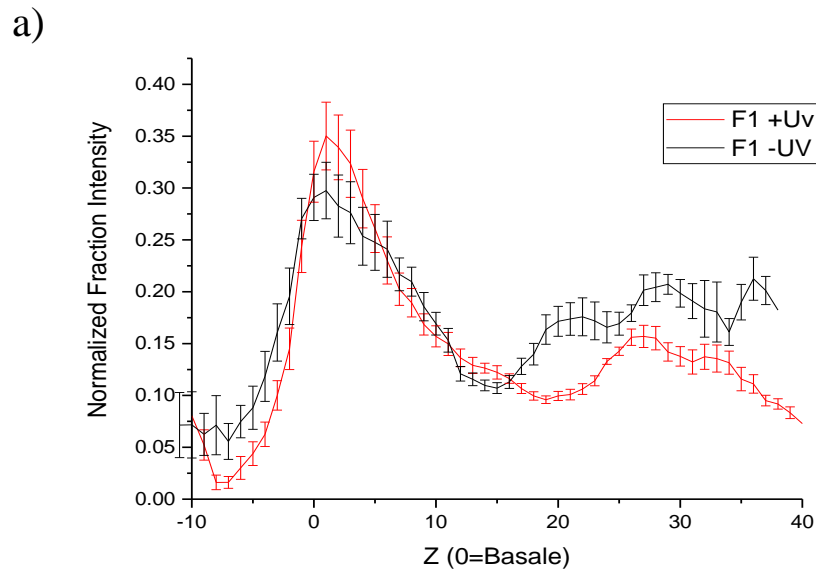
Figure 11 a) The fraction of enol isomer present at various concentrations of SDS after 1200 s of irradiation. b) The fraction of enol isomer present of various surfactants above their CMC after 2400 s of irradiation. *Photochem. Photobiol. Sci.*, 2020,19, 390-398

The micellar encapsulation of AV molecules is important in ensuring the solubility of such particles and the stability of the enol isomer. Figure 11a describes the fraction of enol isomer at 1200 s based on various SDS concentrations above and below the CMC (8 mM). Above the CMC, the data suggests a drastic increase in enol stabilization and minimal diketone formation suggesting the importance of the micelle structure. Forming the micelle provides two major advantages: minimizing the intermolecular interactions between neighboring AV particles and assisting the formation of hydrogen bonds to increase stabilization of the enol form by water. Additionally, the molecular structure of each surfactant contributes to the effectiveness of enol stabilization, independent of the CMC. Specifically, the surfactants SDS, SDBS, and SL were effective in stabilizing AV, while TTAB and CTAB did not stabilize AV to the same extent. The specific properties of surfactants that contribute to the photostability of AV remains unclear. Although, the enhanced stability provided by SDS, SDBS, and SL suggests a negatively charged (anionic) headgroup is a possible molecular property to ensure photostability. Further research must be investigated to understand the reaction mechanisms and to explain the variation of photostability between surfactants.

Goal 2: Test AV/Surfactant Ability to Protect the Skin

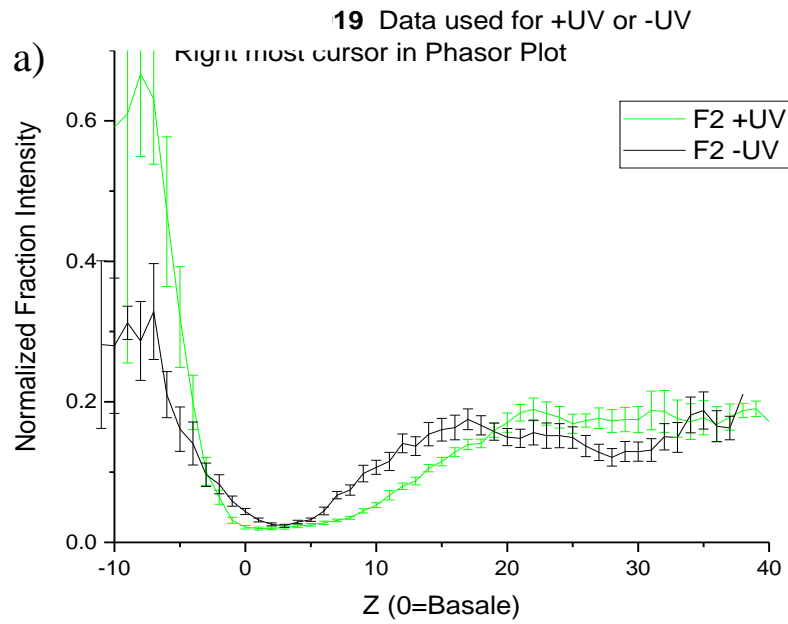
Current and upcoming research investigates the lipid composition and fluidity of the different epidermal layers under UV exposure. Figure 12 illustrates this change in epidermal composition in regard to membrane and cell fluidity. Z corresponds to the layer of the epidermis in accordance to depth with $Z = 0$ being the stratum basale layer, the deepest layer of the epidermis. Therefore, $Z = 35$ corresponds to the stratum granulosum, the top-most layer of the skin containing nuclei. Following UV irradiation, the stratum granulosum experiences a decrease in

membrane fluidity compared to the other epidermal layers. The images illustrate a density of fluidity surrounding the nuclei of the stratum granulosum. This data suggests a drop in



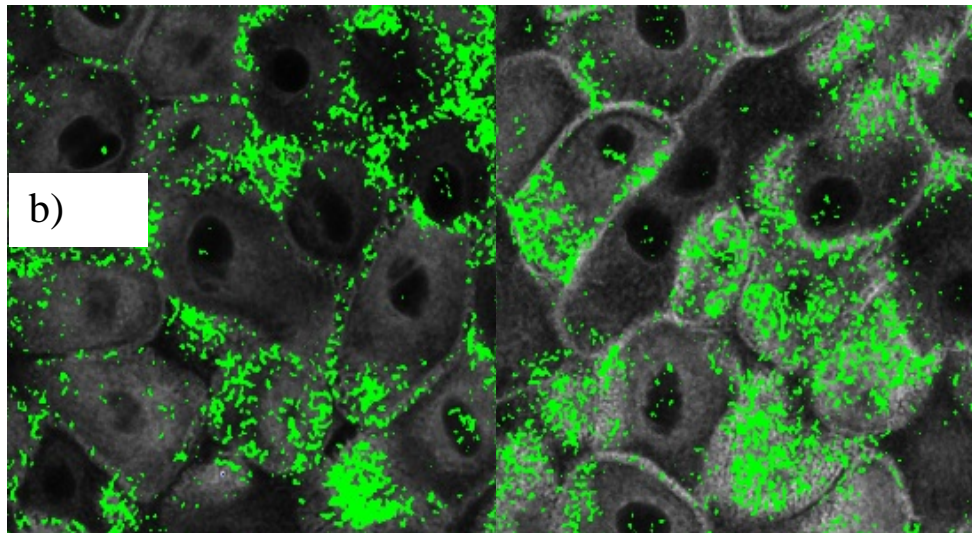
Stratum Granulosum (Z=35)

Figure 12 a) Fractional Intensity measures the fluidity of the area across various layers of the epidermis depth (Z). **b)** Red markers indicate the fluidity of the area before and after UV irradiation.



-UV

+UV



Stratum Granulosum (Z=35)

Figure 13 a) Fractional Intensity measures the rigidity of the area across various layers of the epidermis depth (Z). **b)** Green markers indicate the rigidity of the area before and after UV irradiation.

fluidity surrounding the region of the nuclei, supported by a decrease in red areas on Figure 12b. Possible explanations for this observation may require additional experiments and investigation. Figure 13 illustrates the fractional intensity of rigidity of the epidermal layers when exposed to UV radiation. The green areas tend to be concentrated within the cell membrane and extracellular space. Following UV exposure, the rigidity of the green regions such as the cell membrane, increase in concentration and prominence. Specifically, the image after UV irradiation exhibits a more disorganized nature of how the rigidity regions are dispersed compared to the locality of the rigidity along the cell membrane prior to irradiation. Again, upcoming research would involve understanding how UV radiation alters the fluidity and rigidity of the epidermal layers. The next step of this project will be to use the imaging technique that we developed to test if AV in surfactants will maintain the cell characteristics as seen in the pre-UV irradiated images above.

Conclusion

The findings in this project show that in water, AV undergoes rapid aggregation leading to increased degradation from the UVA absorbing chelated enol tautomer to the UVC absorbing diketone isomer. Because UVC is blocked by the ozone layer, this tautomerization represents a loss of the molecule's ability to act as an efficient sunscreen. The data suggest a possible alternative involves dissolving AV in polar, protic solvents or in biocompatible solvents that incorporate surfactants. The micellar encapsulation of AV by surfactants promotes stability of the chelated keto-enol form and maintains a high photoabsorption of UVA radiation. The intermolecular interactions between the water, surfactant and AV promote isomer stability and minimize any undesirable AV-AV interactions. Further research investigated the composition of

the epidermal layers following UV irradiation, which provides a baseline understanding of what the epidermis looks like before and after UV irradiation for future AV + surfactant protection studies using the same technique. Understanding these research areas can promote the safety and well-being of others through more effective commercial sunscreen and greater awareness on how our skin cells change after UV exposure.

Acknowledgements

This research was heavily supported by the guidance and mentorship of Dr. Christopher J. Bardeen, Dr. Kerry M. Hanson, and the Bardeen Lab. This project was supported by the University Honors Program, the Office of Undergraduate Education, the Research in Science and Engineering Program, the Department of Chemistry, and the National Science Foundation.

References

1. K. M. Hanson, M. Cutuli, T. Rivas, M. Antuna, J. Saoub, N. T. Tierce and C. J. Bardeen, Effects of solvent and micellar encapsulation on the photostability of avobenzone, *Photochem. Photobiol. Sci.*, 2020, 19, 390-398
2. K. M. Hanson, S. Narayanan, V. M. Nichols and C. J. Bardeen, Photochemical degradation of the UV filter octyl methoxycinnamate in solution and in aggregates, *Photochem. Photobiol. Sci.*, 2015, 14, 1607–1616
3. L. A. Baker, S. E. Grennough and V. G. Stavros, A perspective on the ultrafast photochemistry of solution-phase sunscreen molecules, *J. Phys. Chem. Lett.*, 2016, 7, 4655– 4665.
4. R. M. Sayre, J. C. Dowdy, A. J. Gerwig, W. J. Shields and R. V. Lloyd, Unexpected photolysis of the sunscreen octinoxate in the presence of the sunscreen avobenzone, *Photochem. Photobiol.*, 2005, 81, 452–456.
5. R. Stokes and B. Diffey, In vitro assessment of sunscreen photostability: the effect of radiation source, sunscreen application thickness and substrate, *Int. J. Cosmet. Sci.*, 1999, 21, 341–351.
6. D. Dondi, A. Albini and N. Serpone, Interactions between different solar UVB/UVA filters contained in commercial sunscreens and consequent loss of UV protection, *Photochem. Photobiol. Sci.*, 2006, 5, 835–843.
7. G. J. Mturi and B. S. Martinicigh, Photostability of the sun- screening agent 4-tert-butyl-4'-methoxydibenzoylmethane (avobenzone) in solvents of different polarity and proticity, *J. Photochem. Photobiol.*, A, 2008, 200, 410–420.

8. C. A. Bonda, A. Pavlovic, K. M. Hanson and C. J. Bardeen, Singlet quenching proves faster is better for photostability, *Cosmet. Toiletries*, 2010, 125, 40–48.
9. P. M. Farr and B. L. Diffey, The erythral response of human skin to ultraviolet radiation, *Br. J. Dermatol.*, 1985, 113, 65–76.
10. Sunscreen Drug Products for Over-the-Counter Use: Final Rule and Proposed Rules, Food and Drug Administration, Department of Health and Human Services, 2011, vol. 76, pp. 35620–35665,.
11. M. P. Kojic and M. Etinski, A new insight into the photochemistry of avobenzone in gas phase and acetonitrile from ab initio calculations, *Phys. Chem. Chem. Phys.*, 2016, 18, 22168–22178.
12. S. P. Huong, V. Andriew, J.-P. Reynier, E. Rocher and J.-D. Fourneeron, The photoisomerization of the sunscreen ethylhexyl p-methoxy cinnamate and its influence on the sun protection factor, *J. Photochem. Photobiol., A*, 2007, 186, 65–70.